

Two-phonon  $\gamma$ -vibrational strength in osmium nuclei

C. Y. Wu, D. Cline, A. B. Hayes, and M. W. Simon

*Nuclear Structure Research Laboratory, Department of Physics, University of Rochester, Rochester, New York 14627*

R. Krücken, J. R. Cooper, C. J. Barton, C. W. Beausang, C. Bialik, M. A. Caprio, R. F. Casten, A. A. Hecht, H. Newman, J. Novak, N. Pietralla, K. Zyromski, and N. V. Zamfir\*

*A. W. Wright Nuclear Structure Laboratory, Yale University, New Haven, Connecticut 06520*

(Received 22 February 2001; published 5 June 2001)

Collective  $E2$  strengths were measured to probe the two-phonon  $\gamma$ -vibrational character of  $I_K^\pi = 4_4^+$  states for  $^{188,190}\text{Os}$ . Lifetimes for states with spin up to  $8^+$  of the ground-state band,  $6^+$  of the  $\gamma$  band, and the  $4^+$  state of the  $K^\pi = 4^+$  band were measured by the recoil-distance method following Coulomb excitation by a  $^{58}\text{Ni}$  projectile at  $E_{\text{lab}} = 275$  MeV. These lifetime data are compared with the electromagnetic matrix elements measured by previous Coulomb excitation experiments. The good agreement between these independent measurements supports the conclusion, made by the Coulomb excitation work, that the electromagnetic properties of these osmium nuclei are consistent with the description of  $\gamma$ -soft collective models. In addition, it supports the evidence that the two-phonon  $\gamma$ -vibration configuration is the dominant component for the lowest-lying  $I_K^\pi = 4_4^+$  states in osmium nuclei.

DOI: 10.1103/PhysRevC.64.014307

PACS number(s): 21.10.Re, 21.10.Tg, 27.70.+q

Experimental evidence for the existence of two-phonon  $\gamma$ -vibrational states ( $I^\pi = 4^+$  and  $K = 4$ ) in osmium isotopes was suggested long ago by Yates *et al.* [1] as well as by Casten and Cizewski [2]. Their evidence includes the facts that the measured level energies lie at about twice that of the one-phonon state, and that the decay branching ratios suggest forbiddance for the decay from the two-phonon state to the zero-phonon state. However, these are necessary, but not sufficient, conditions. For example, weak transitions to the ground-state band are expected due to the  $K$  forbiddance regardless of the detailed structure of the  $I_K^\pi = 4_4^+$  state. The strongest evidence supporting the existence of a two-phonon assignment is provided by Coulomb excitation work [3], which measured enhancement of the  $B(E2)$  values for decay of the  $I_K^\pi = 4_4^+$  states to the one  $\gamma$ -phonon band states ranging up to 47 Weisskopf units, while the  $B(E2)$  values to the ground band are 200 to 1000 times weaker. In addition, the ratios of the intrinsic  $E2$  matrix elements between the two-phonon excitation and the one-phonon excitation approach the harmonic vibrator limit [4]. The intrinsic matrix elements were derived from the measured electromagnetic matrix elements [3] after correcting for the coupling between the rotational and intrinsic motions [5].

The measured  $E2$  properties appear to conflict with other data. Significant  $E4$  strengths coupling the ground state to the first  $I_K^\pi = 4_4^+$  states in  $^{188,190,192}\text{Os}$ , measured by the  $(\alpha, \alpha')$  reaction [6,7] and  $(p, p')$  reaction [8], suggests the importance of the hexadecapole degree of freedom in those states. Also, significant two-quasiparticle components in the  $I_K^\pi = 4_4^+$  states of  $^{190,192}\text{Os}$  were suggested by studies of the  $(t, \alpha)$  reaction [9]. Admixtures of nearly 50% of the  $5/2^+[402] + 3/2^+[402]$  two-quasiproton configurations were implied for the  $I_K^\pi = 4_4^+$  states in  $^{190,192}\text{Os}$  [10], which may be

consistent with the finding of the hexadecapole components in those states. The apparent conflict, based on the notion that dominant single-particle configurations should be absent in collective states, between the results of the Coulomb excitation work and the light-ion induced experiments certainly justifies further experimental and theoretical study. In this paper, we report on an experimental study of the electromagnetic properties of the first  $I_K^\pi = 4_4^+$  states in  $^{188,190}\text{Os}$  using the recoil distance method (RDM) [11–13].

The RDM lifetime measurements were carried out using the New Yale Plunger Device (NYPD) [14] at the Wright Nuclear Structure Laboratory of Yale University. The osmium nuclei were Coulomb excited using a  $^{58}\text{Ni}$  beam at  $E_{\text{lab}} = 275$  MeV provided by the Yale ESTU tandem accelerator. The targets were  $\approx 360$   $\mu\text{g}/\text{cm}^2$  thick isotopically enriched osmium isotopes sputtered onto nickel backing foils having a thickness  $\approx 500$   $\mu\text{g}/\text{cm}^2$ . The deexcitation  $\gamma$  rays were detected by the SPEEDY array [15] consisting of seven segmented clover Ge detectors, plus one  $\approx 70\%$  Ge detector, all in coincidence with the backscattered particles detected by an array of solar cells covering an angular range from  $153^\circ$  to  $171^\circ$ . The detection efficiency of the Ge and clover detectors was measured using  $^{133}\text{Ba}$  and  $^{152}\text{Eu}$  radioactive sources.

For both the  $^{188}\text{Os}$  and  $^{190}\text{Os}$  experiments, the forward recoiling osmium nuclei had an initial velocity  $v/c = 0.043(1)$  after leaving the nickel backing and subsequently were slowed down to  $v/c = 0.027(1)$  by a  $\approx 2.8$   $\text{mg}/\text{cm}^2$  thick nickel velocity-shifter foil. This velocity shift allows a sufficient separation of the Doppler shifted  $\gamma$ -ray energies of the fast and slow components, that is, those decaying prior to and those decaying after passing through the velocity-shift foil, for any given  $\gamma$ -ray transitions of osmium nuclei. The initial recoil velocity was determined from the comparison between the shifted and zero-shifted  $\gamma$ -ray energies. The latter was measured separately using a  $\approx 11.3$   $\text{mg}/\text{cm}^2$  thick

\*Present address: Clark University, Worcester, MA 01610.

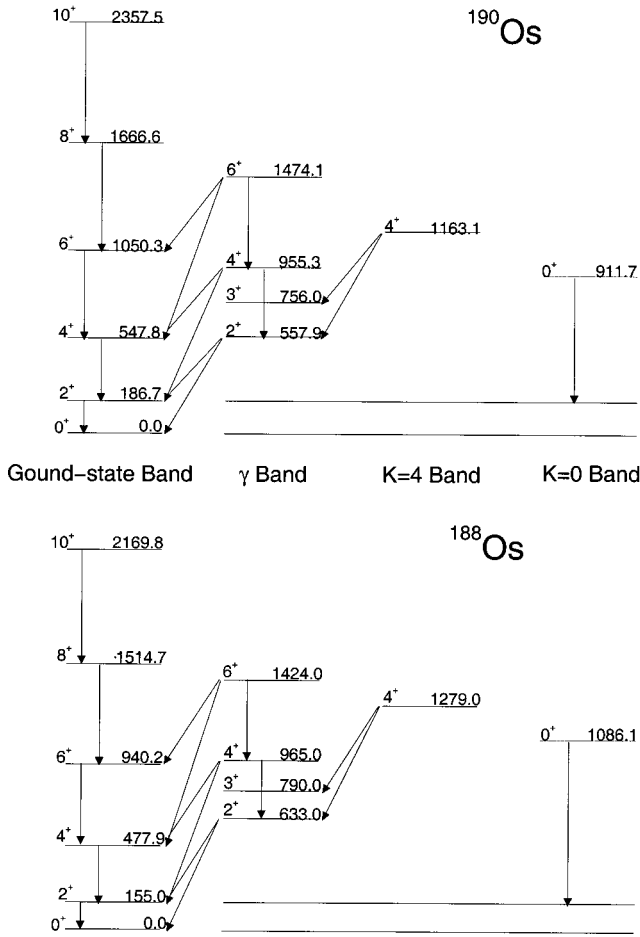


FIG. 1. Partial level schemes and the  $\gamma$ -ray transitions observed in this work for  $^{188,190}\text{Os}$ . Level energies are in keV.

nickel foil in place of the velocity-shift foil to fully stop the recoiling osmium nuclei. The recoil distance measurements were made at six distances, varying from 10 to 311  $\mu\text{m}$ , between the target and the velocity-shifter foil. In addition, measurements also were made at three large distances between 2000 and 8000  $\mu\text{m}$ . The distance was adjusted by moving the target foil through the contraction and expansion of a series of piezoelectrical crystals controlled by a Burleigh 6000ULN unit. During the measurement, the distance was kept constant to better than 3% by a feedback system to continuously monitor the capacitance of the target-foil parallel system against the preset value [14]. The distance calibration was made by measuring the capacitance of the target-foil parallel system against a micrometer reading. The capacitance is inversely proportional to its separation at distances sufficiently small relative to the dimensions of the foil surface.

The partial level schemes for  $^{188,190}\text{Os}$  pertaining to this work are shown in Fig. 1. States with spin up to  $10^+$  of the ground-state band,  $6^+$  of the  $K=2$ ,  $\gamma$ -vibrational band, and  $4^+$  of the  $K=4$ , suggested two-phonon  $\gamma$ -vibrational band were populated by Coulomb excitation for both osmium isotopes. The data from the  $0^\circ$  clover detector were used to determine the lifetimes using the method described in the following paragraph. Examples of the  $\gamma$ -ray spectra for three

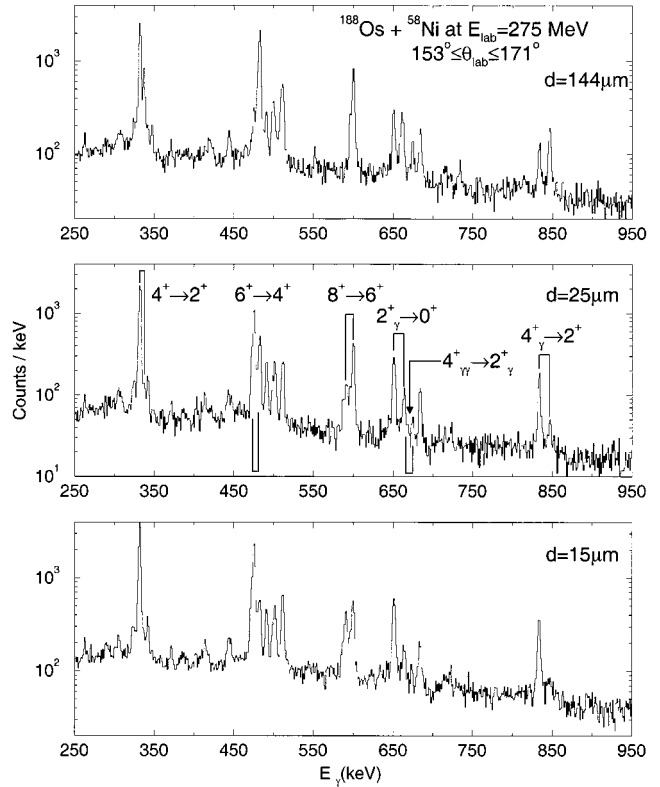


FIG. 2. The  $\gamma$ -ray spectra of  $^{188}\text{Os}$  from the clover detector at  $0^\circ$ , the beam direction. The fast and slow components for each  $\gamma$ -ray transition are indicated by the thick lines and their relative intensities variations from one distance to another are visible.

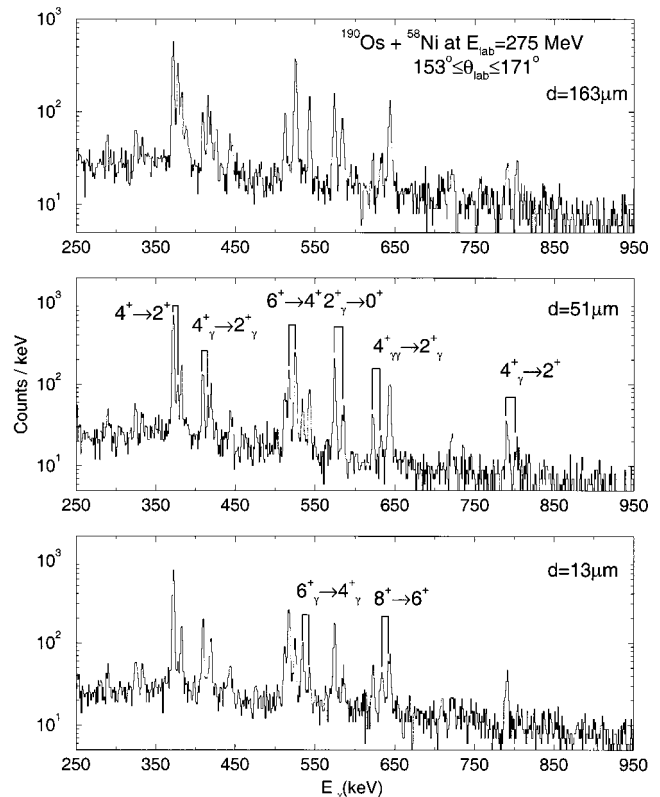


FIG. 3. The same as in Fig. 2 but for  $^{190}\text{Os}$ .

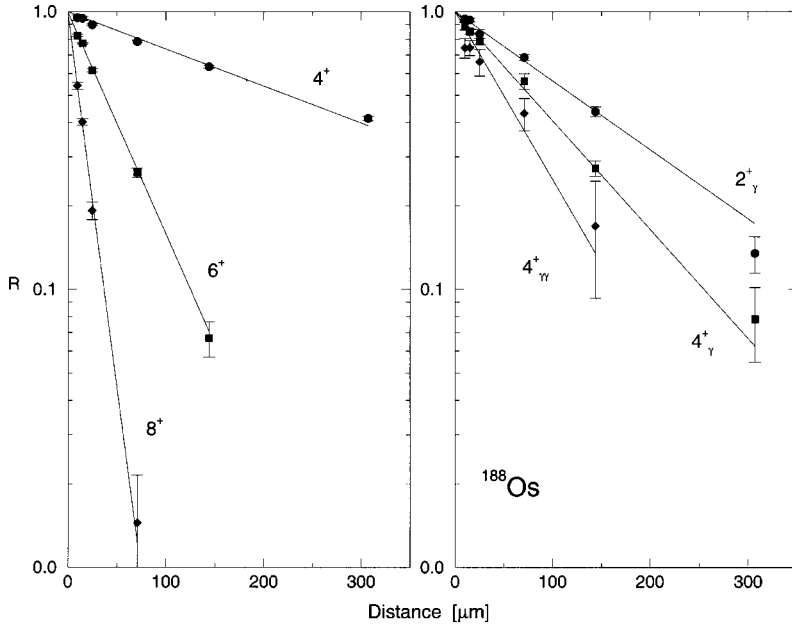


FIG. 4. The ratio of the slow component to the total, slow+fast, as a function of distance between the target and the velocity-shift foil for  $^{188}\text{Os}$ . These data have been corrected for the feeding and other effects mentioned in the text. The best fit to the data are shown as the solid lines with the extracted lifetimes listed in Table I.

different distances are shown in Figs. 2 and 3 for  $^{188,190}\text{Os}$ , respectively.

In the recoil distance method, the lifetime is determined from the intensity ratio  $R$  of the slow component to the total, that is, the slow component plus the fast component. To a first-order approximation,  $R$  is related to the mean lifetime  $\tau$  by  $R = \exp(-d/v\tau)$ , where  $d$  is the distance between the tar-

get and the velocity-shifter foil and  $v$  is the initial recoil velocity. A modified version [16,17] of the code ORACLE [18] was used to extract the lifetimes. It takes into account the feeding to the level of interest, which is calculated initially using the electromagnetic matrix elements from the Coulomb excitation experiments [3], the different solid angles, the detection efficiency of the slow and fast compo-

TABLE I. Comparison of the mean lifetimes and the  $B(E2)$  values of excited states determined from both the Coulomb excitation work cited in Ref. [3] (Coulex) and the direct lifetime measurement of this work for  $^{188}\text{Os}$ .

State	Transition	$E_\gamma$ (keV)	$\tau_{\text{exp}}$ (ps)		$B(E2)(e^2 \text{ b}^2)$	
			Coulex	this work	Coulex	this work
$2_1^+$	$2_1^+ \rightarrow 0_1^+$	155.0	1001(13)	930(140)	0.502(6)	0.540(81)
$4_1^+$	$4_1^+ \rightarrow 2_1^+$	322.9	28.0(5)	25.5(14)	0.776(15)	0.852(47)
$6_1^+$	$6_1^+ \rightarrow 4_1^+$	462.3	4.48(11)	4.25(24)	0.843(20)	0.888(50)
$8_1^+$	$8_1^+ \rightarrow 6_1^+$	574.5	1.39(8)	1.27(8)	0.927(51)	1.01(6)
$2_2^+$ ( $K=2$ )			9.47(22)	13.6(15) <sup>a</sup>		
	$2_2^+ \rightarrow 0_1^+$	633.0			0.0467(17)	0.0325(36)
	$2_2^+ \rightarrow 2_1^+$	478.0			0.150(4)	0.104(11)
$4_2^+$ ( $K=2$ )			9.16(32)	8.68(76) <sup>b</sup>		
	$4_2^+ \rightarrow 2_1^+$	810.0			0.0089(5)	0.0094(10)
	$4_2^+ \rightarrow 4_1^+$	487.1			0.134(7)	0.140(14)
	$4_2^+ \rightarrow 2_2^+$	332.0			0.352(28)	0.371(44)
$4_3^+$ ( $K=4$ )			4.77(53)	5.6(12) <sup>c</sup>		
	$4_3^+ \rightarrow 2_1^+$	1124.0			0.0017(6)	0.0014(6)
	$4_3^+ \rightarrow 2_2^+$	646.0			0.0765(74)	0.065(15)
	$4_3^+ \rightarrow 3_1^+$	489.0			0.152(44)	0.129(47)
	$4_3^+ \rightarrow 4_2^+$	314.0			0.299(26)	0.255(59)

<sup>a</sup>From the  $2_2^+ \rightarrow 0_1^+$  transition.

<sup>b</sup>From the  $4_2^+ \rightarrow 2_1^+$  transition.

<sup>c</sup>From the  $4_3^+ \rightarrow 2_2^+$  transition.

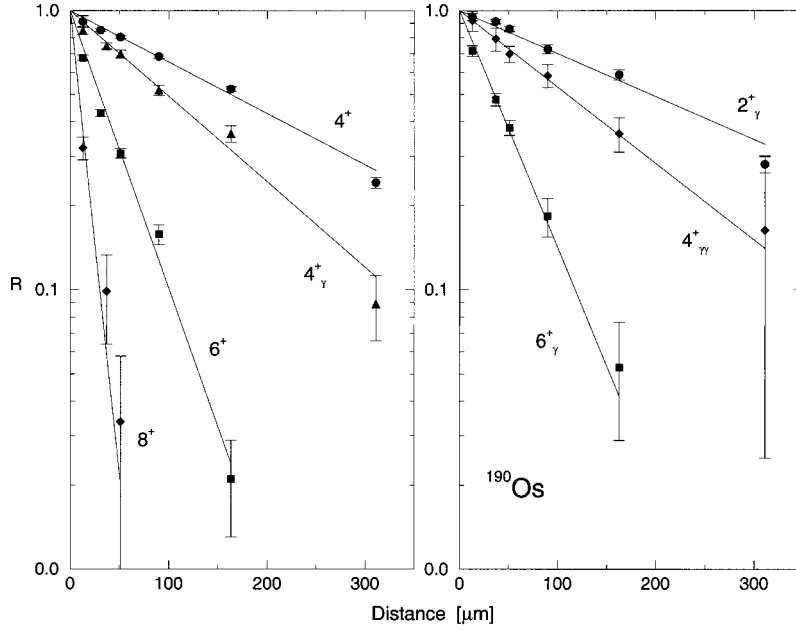


FIG. 5. The same as in Fig. 4 but for  $^{190}\text{Os}$  and the extracted lifetimes are listed in Table II.

nents for a given  $\gamma$ -ray transition, and the deorientation effect. Iterations were followed until convergence was achieved by changing the feeding according to the set of electromagnetic matrix elements derived from the extracted lifetimes. The treatment of the deorientation effect, and its

influence on the extracted lifetime in the modified code, is discussed in Refs. [17,19]. Other major changes in the modified code are (1) the Bateman equations for handling the single cascade feeding are replaced by a numerical method that tracks the populations of excited states as a function of

TABLE II. The same as Table I but for  $^{190}\text{Os}$ .

State	Transition	$E_\gamma$ (keV)	$\tau_{\text{exp}}$ (ps)		$B(E2)(e^2 \text{ b}^2)$	
			Coulex	this work	Coulex	this work
$2_1^+$	$2_1^+ \rightarrow 0_1^+$	186.7	542(14)	540(36)	0.468(12)	0.470(31)
$4_1^+$	$4_1^+ \rightarrow 2_1^+$	361.1	20.4(14)	18.4(10)	0.623(42)	0.691(38)
$6_1^+$	$6_1^+ \rightarrow 4_1^+$	502.5	3.69(16)	3.40(20)	0.679(29)	0.737(43)
$8_1^+$	$8_1^+ \rightarrow 6_1^+$	616.3	1.12(6)	1.02(14)	0.814(44)	0.89(12)
$2_2^+$ ( $K=2$ )			21.2(8)	22.0(20) <sup>a</sup>		
	$2_2^+ \rightarrow 0_1^+$	557.9			0.0394(15)	0.0380(38)
	$2_2^+ \rightarrow 2_1^+$	371.2			0.227(16)	0.219(25)
$4_2^+$ ( $K=2$ )			9.88(32)	11.1(9) <sup>b</sup>		
	$4_2^+ \rightarrow 2_1^+$	768.6			0.00458(32)	0.00408(43)
	$4_2^+ \rightarrow 4_1^+$	407.5			0.229(14)	0.204(21)
	$4_2^+ \rightarrow 2_2^+$	397.4			0.389(17)	0.346(32)
$6_2^+$ ( $K=2$ )			3.12(37)	4.01(36) <sup>c</sup>		
	$6_2^+ \rightarrow 4_1^+$	926.3			0.0029(22)	0.0023(18)
	$6_2^+ \rightarrow 6_1^+$	423.8			0.238(54)	0.185(45)
	$6_2^+ \rightarrow 4_2^+$	518.8			0.520(64)	0.405(61)
$4_3^+$ ( $K=4$ )			9.0(12)	12.4(23) <sup>d</sup>		
	$4_3^+ \rightarrow 2_1^+$	976.4			0.00030(8)	0.00020(7)
	$4_3^+ \rightarrow 2_2^+$	605.2			0.0659(86)	0.048(11)
	$4_3^+ \rightarrow 3_1^+$	407.1			0.267(86)	0.194(72)
	$4_3^+ \rightarrow 4_2^+$	207.8			0.281(39)	0.204(47)

<sup>a</sup>From the  $2_2^+ \rightarrow 0_1^+$  transition.  $\tau=22.2(45)$  ps from the  $2_2^+ \rightarrow 2_1^+$  transition.

<sup>b</sup>From the  $4_2^+ \rightarrow 2_2^+$  transition.  $\tau=13.6(24)$  ps from the  $4_2^+ \rightarrow 2_1^+$  transition.

<sup>c</sup>From the  $6_2^+ \rightarrow 4_2^+$  transition.

<sup>d</sup>From the  $4_3^+ \rightarrow 2_2^+$  transition.

time from time zero for every 1/100 ps step and (2) multiple decay paths allow handling of more than one decay branch for the excited states.

The  $^{188}\text{Os}$  data, corrected for the feeding and the effects mentioned above, are shown in Fig. 4 as a function of target-shifter separation distance  $d$  together with the best fit indicated by the straight lines. The extracted lifetimes, and the comparison with those inferred from the electromagnetic matrix elements measured by the Coulomb excitation experiments, are listed in Table I. The internal conversion coefficients, used to derive the lifetimes from the matrix elements, were determined with the tables listed in Ref. [20]. The individual matrix elements, derived from the measured lifetimes and the known branching ratios, also are listed in Table I. The same are shown for  $^{190}\text{Os}$  in Fig. 5 and listed in Table II. Except for the  $2^+$  and  $4^+$  states of the  $\gamma$  band in  $^{190}\text{Os}$ , where the lifetimes were determined from two decay branches, the lifetimes for other members of the  $K=2$  and 4 bands were determined by only one decay branch because the other branches were either too weak or were contaminated by other transitions. For the same reasons it was not possible to determine the lifetime for the  $6^+$  state of the  $\gamma$  band in  $^{188}\text{Os}$  for the present experiment. The accuracy for the extracted lifetimes typically is better than 10%, which is consistent with the quality of earlier work with the Rochester plunger [17,19]. These extracted lifetimes are in good agreement with those independently determined by the differential decay-curve method [21,22] on the same set of data for all three Ge detector angles [23].

Measurements of Coulomb excitation yields, induced by heavy-ion beam, are a powerful probe of electromagnetic matrix elements for low-lying collective bands in nuclei. The analysis of such data involves a global least squares fit of the relative signs and magnitudes of many electromagnetic matrix elements to a large data set using the Coulomb excitation search code GOSIA [24]. Direct lifetime measurements, using the recoil distance method, for many states in  $^{110}\text{Pd}$  [19],  $^{148}\text{Nd}$  [25],  $^{165}\text{Ho}$  [26],  $^{166}\text{Er}$  [27],  $^{168}\text{Er}$  [28], and  $^{182,184}\text{W}$  [29] have been found to be in good agreement with lifetimes derived from the electromagnetic matrix elements extracted from the analysis of Coulomb excitation yield data. This fact provides convincing support for the reliability and accuracy of the Coulomb excitation yield analysis technique. Similarly, the agreement between the Coulomb excitation yield and recoil distance lifetime measurements for the present work, shown in Tables I and II, is generally within 10–20% for 14 states, supporting the conclusions on the collective characters of the investigated states made in Ref. [3]. Note that pure  $E2$  transitions were assumed for the decay of the  $I_K^\pi=4_4^+$  state while the  $E2/M1$  mixing ratios for the decay of the  $\gamma$  band members were measured [3]. The present recoil distance lifetime measurements for the  $I_K^\pi=4_4^+$  states of interest are about 20% longer than implied by the earlier Coulomb excitation study for both nuclei. There is a significant disagreement for the second  $2^+$  state in  $^{188}\text{Os}$ , where the directly measured lifetime is  $\approx 44\%$  longer than that derived from all the early Coulomb excitation work [30,31,3]. It is still unclear what is the reason for this discrepancy.

The osmium nuclei are located in a prolate to oblate shape

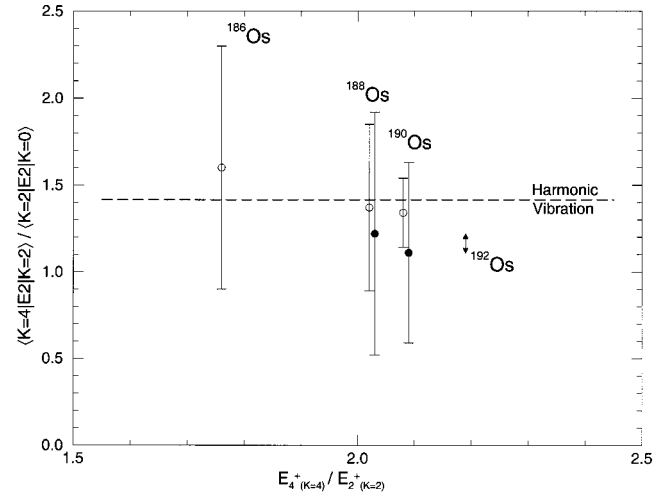


FIG. 6. Ratios of the intrinsic quadrupole matrix element of the two-phonon excitation to the one-phonon excitation plotted vs the ratios of their excitation energies. The intrinsic quadrupole matrix elements were derived from the measured interband electromagnetic matrix elements after correcting the coupling between the rotational and intrinsic motions. The open circles are the results from the Coulomb excitation measurement and the filled ones are the results from the lifetime measurement. The dashed line is the harmonic vibration limit for the two-phonon relative to the one-phonon strength. The double-sided arrow marked for  $^{192}\text{Os}$  shows the range of values determined by a three-band mixing calculation (ground state  $\gamma$  and  $K=4$  bands).

transition region reflecting the importance of the  $\gamma$  degree of freedom. This provides an opportunity to address issues related to this collective degree of freedom, such as the  $\gamma$  softness and the two-phonon  $\gamma$  vibration. The measurement of the electromagnetic matrix elements to the  $\gamma$  band or the one-phonon  $\gamma$  vibration, is generally a measure of the central value of the  $\gamma$  degree of freedom. To measure the  $\gamma$  softness, that is variance, one has to measure the electromagnetic matrix elements at least to the two-phonon excitation [32–34]. The identification of the  $I_K^\pi=4_4^+$  state as the two-phonon  $\gamma$  vibration is strongly supported by the enhanced  $B(E2)$  values, which range up to 47 Weisskopf units (1 W.u.=0.0064  $e^2 b^2$ ), measured by Coulomb excitation for the transition to the  $4^+$  of the  $\gamma$  band in  $^{188}\text{Os}$ , the inhibited  $B(E2)$  values to the ground band which are 200 to 1000 times weaker, the positive static moment of the  $I_K^\pi=4_4^+$  state [3], and the almost harmonic excitation energies [1,2]. Comparisons of these  $E2$  matrix elements directly to collective model predictions, or variances determined by using the rotational-invariant technique [32,33], both imply the importance of the  $\gamma$ -soft degree of freedom.

To ascertain the purity of the two-phonon  $\gamma$ -vibration configuration in the  $I_K^\pi=4_4^+$  state, one has to study the electromagnetic properties in the intrinsic frame because the interpretation of the interband matrix elements invokes a strong coupling between the rotational and intrinsic motions. The intrinsic matrix elements for the phonon strengths can be derived after removing the effects of that coupling [4]. Ratios of the intrinsic quadrupole matrix element of the two-



phonon excitation to the one-phonon excitation vs ratios of their excitation energies, deduced from both the lifetime and Coulomb excitation yield analyses, are shown in Fig. 6 for the osmium isotopes. Within the experimental uncertainties, all ratios of the intrinsic  $E2$  matrix elements are consistent with a two- $\gamma$ -phonon interpretation for the lowest-lying  $I_K^\pi = 4_4^+$  states in  $^{186,188,190,192}\text{Os}$ . Upper limits for the deviation from the harmonic two-phonon  $\gamma$ -vibration strength, from both sets of results, imply that admixtures of components other than two-phonon  $\gamma$ -vibration component must be no more than  $\approx 25\%$  in the wave functions of the  $I_K^\pi = 4_4^+$  states in these osmium nuclei. This is only half of the admixture implied by an analysis of  $(t, \alpha)$  reaction strengths [10], assuming that all of the admixture is attributed to the  $5/2^+[402] + 3/2^+[402]$  two-quasiproton configuration. The present work confirms the strong enhanced  $B(E2)$  collectivity, the branching ratios, and the excitation energies, all of which are consistent with a large two-phonon  $\gamma$ -vibration component in the structure of the  $I_K^\pi = 4_4^+$  states. We stress that these results are not inconsistent with weak admixtures of hexadecapole excitations, or the  $5/2^+[402] + 3/2^+[402]$

two-quasiproton configuration, but seem to be incompatible with the strength inferred from the  $(t, \alpha)$  reaction strengths [10].

In summary, lifetime measurements for the low-lying collective states in  $^{188,190}\text{Os}$  have been performed using the recoil distance method. The measured lifetimes confirm the  $E2$  properties derived from prior heavy-ion induced Coulomb excitation experiments. Both the Coulomb excitation yield and the recoil distance lifetime measurements unambiguously determine highly enhanced  $E2$  transition strengths between the  $I_K^\pi = 4_4^+$  band heads and the one  $\gamma$ -phonon bands. These results imply that the two-phonon  $\gamma$ -vibration component must dominate the wave functions of the  $I_K^\pi = 4_4^+$  states in osmium nuclei, which is somewhat in conflict with the structure implied by light-ion transfer reactions.

We express our thanks to the WNSL accelerator staff for their excellent performance. The work at Rochester was supported by U.S. NSF, at Yale by the U.S. DOE under Grant No. DOE-FG02-91ER-40609 as well as by the German DFG under Grant No. Pi393/1-1, and at Clark by the U.S. DOE under Grant No. DE-FG02-88ER-40417.

- 
- [1] S.W. Yates, J.C. Cunnane, R. Hochel, P.J. Daly, R. Thompson, and R.K. Sheline, *Nucl. Phys.* **A222**, 276 (1974); S.W. Yates *et al.*, *ibid.* **A222**, 301 (1974).
- [2] R.F. Casten and J.A. Cizewski, *Nucl. Phys.* **A309**, 477 (1978); **A425**, 653 (1984).
- [3] C.Y. Wu, D. Cline, T. Czosnyka, A. Backlin, C. Baktash, R.M. Diamond, G.D. Dracoulis, L. Hasselgren, H. Kluge, B. Kotlinski, J.R. Leigh, J.O. Newton, W.P. Phillips, S.H. Sie, J. Srebrny, and F.S. Stephens, *Nucl. Phys.* **A607**, 178 (1996).
- [4] C.Y. Wu and D. Cline, *Phys. Lett. B* **382**, 214 (1996).
- [5] A. Bohr and B.R. Mottleson, *Nuclear Structure*, Vol. II (Benjamin, Reading, MA, 1975).
- [6] D.G. Burke, M.A.M. Shahabuddin, and R.N. Boyd, *Phys. Lett.* **78B**, 48 (1978).
- [7] F.T. Baker, M.A. Grimm, Jr., A. Scott, R.C. Styles, T.H. Kruse, J. Jones, and R. Suchanek, *Nucl. Phys.* **A371**, 68 (1981).
- [8] F.T. Baker, A. Sethi, V. Penumetcha, G.T. Emery, W.P. Jones, M.A. Grimm, and M.L. Whiten *Phys. Rev. C* **32**, 2212 (1985); *Nucl. Phys.* **A501**, 546 (1989).
- [9] R.D. Bagnell, Y. Tanaka, R.K. Sheline, D.G. Burke, and J.D. Sherman, *Phys. Lett.* **66B**, 129 (1977); *Phys. Rev. C* **20**, 42 (1979).
- [10] D.G. Burke, *Phys. Lett. B* **406**, 200 (1997); *Phys. Rev. Lett.* **73**, 1899 (1994).
- [11] T.K. Alexander and A. Bell, *Nucl. Instrum. Methods* **81**, 22 (1970).
- [12] N. Anyas-Weiss, R. Griffiths, N.A. Jelley, W. Randolph, J. Szucs, and T.K. Alexander, *Nucl. Phys.* **A201**, 513 (1973).
- [13] M.W. Guidry, R.J. Sturm, N.R. Johnson, E. Eichler, G.D. O'Kelley, N.C. Singhal, and R.O. Sayer, *Phys. Rev. C* **13**, 1164 (1976).
- [14] R. Krücken, in *Proceedings of the International Conference on Perspectives in Nuclear Physics*, edited by J.H. Hamilton, H.K. Carter, and R.B. Piercey (World Scientific, Singapore, 1999), p. 111.
- [15] R. Krücken, *Proceedings of the International Conference on Applications of Accelerator in Research and Industry*, 2000 (to be published).
- [16] C.Y. Wu, B. Kotlinski, D. Cline, and M.W. Simon (unpublished).
- [17] C.Y. Wu, *J. Res. Natl. Inst. Stand. Technol.* **105**, 63 (2000).
- [18] R.J. Sturm and M.W. Guidry, *Nucl. Instrum. Methods* **138**, 345 (1976).
- [19] B. Kotlinski, D. Cline, A. Backlin, and D. Clark, *Nucl. Phys.* **A503**, 575 (1989).
- [20] F. Rosel, H.M. Fries, K. Alder, and H.C. Pauli, *At. Data Nucl. Data Tables* **21**, 291 (1978).
- [21] A. Dewald, S. Harissopulos, and P. von Brentano, *Z. Phys. A* **334**, 163 (1989).
- [22] G. Böhm, A. Dewald, P. Petkov, and P. von Brentano, *Nucl. Instrum. Methods Phys. Res. A* **329**, 248 (1993).
- [23] C. Bialik, Senior thesis, Yale University, 2001.
- [24] T. Czosnyka, D. Cline, and C.Y. Wu, *GOSIA users manual UR-NSRL-305*, 1991.
- [25] R. Ibbotson, B. Kotlinski, D. Cline, K.G. Helmer, A.E. Kavka, A. Renalds, E.G. Vogt, P.A. Butler, C.A. White, R. Wadsworth, and D.L. Watson, *Nucl. Phys.* **A530**, 199 (1991).
- [26] M.W. Simon *et al.* (unpublished).
- [27] I. Thorslund, C. Fahlander, A. Backlin, B. Kotlinski, D. Cline, A. Renalds, and E.G. Vogt, *Z. Phys. A* **342**, 35 (1992).
- [28] B. Kotlinski, D. Cline, A. Backlin, K.G. Helmer, A.E. Kavka, W.J. Kernan, E.G. Vogt, C.Y. Wu, R.M. Diamond, A.O. Macchiavelli, and M.A. Deleplanque, *Nucl. Phys.* **A517**, 365 (1990).
- [29] C.Y. Wu, D. Cline, E.G. Vogt, W.J. Kernan, T. Czosnyka, K.G. Helmer, R.W. Ibbotson, A.E. Kavka, B. Kotlinski, and R.M. Diamond, *Nucl. Phys.* **A533**, 359 (1991).

- [30] R.F. Casten, J.S. Greenberg, S.H. Sie, G.A. Burginyon, and D.A. Bromley, *Phys. Rev.* **187**, 1532 (1969).
- [31] W.T. Milner, F.K. McGowan, R.L. Robinson, P.H. Stelson, and R.O. Sayer, *Nucl. Phys.* **A177**, 1 (1971).
- [32] D. Cline and C. Flaum (unpublished).
- [33] D. Cline, *Annu. Rev. Nucl. Part. Sci.* **36**, 683 (1986).
- [34] V. Werner, N. Pietralla, P. von Brentano, R.F. Casten, and R.V. Jolos, *Phys. Rev. C* **61**, 021301(R) (2000).